RSC Applied Polymers

ROYAL SOCIETY OF CHEMISTRY

PAPER

View Article Online
View Journal | View Issue

Cite this: *RSC Appl. Polym.*, 2026, **4**, 591

High-refractive-index copolymers produced by radical copolymerization of aromatic heterocyclic monomers in deep eutectic solvents

Yuji Tsuhara,[a] Kento Sato,[a] Sadaki Samitsu [b] and Hideharu Mori *[a]

The development of a greener and more efficient methodology for simultaneously achieving polymers with a high refractive index, high Abbe number, good transparency, and high thermal stability remains a challenge, particularly for sustainable production using environmentally friendly solvents. Herein, we report the green production of high-refractive-index copolymers in a deep eutectic solvent (DES) by the radical copolymerization of aromatic heterocyclic *S*-vinyl and *N*-vinyl monomers, namely benzothiazoyl vinyl sulfide (BTVS) and *N*-vinyl carbazole (NVC), combined with methyl methacrylate (MMA). Three hydrophobic natural DESs (NADESs; Thy/Cou, Thy/Men, and Tdc/Men) prepared from naturally derived compounds (Thy: thymol, Men: (±)-menthol, Cou: coumarin, and Tdc: 1-tetradecanol) and two hydrophilic DESs prepared from choline chloride (ChCl) and zinc chloride ($ZnCl_2$) with urea (ChCl/urea and $ZnCl_2$/urea) were used for the radical copolymerization of MMA/BTVS, MMA/NVC, and BTVS/NVC. An increase in both the polymer yield and molecular weight of the resulting copolymers was observed, depending on the nature of the DESs and the polymerization conditions. P(BTVS-*co*-NVC)s prepared at a constant feed ratio (100/100) in the DESs exhibited high refractive indices (1.6738–1.7359 at 589 nm), which were higher than those of P(MMA-*co*-BTVS)s (1.6076–1.6794) and P(MMA-*co*-NVC)s (1.5922–1.6349). Three series of the copolymers showed good transparency (>96% at 400 nm) and high thermal stability (T_{d5} = 378 °C, 249 °C, and 246 °C for MMA/NVC, MMA/BTVS, and BTVS/NVC copolymers, respectively). P(BTVS-*co*-NVC) prepared at a suitable BTVS/NVC (150/50) feed ratio in $ZnCl_2$/urea showed the highest refractive index (1.7528) with a relatively high Abbe number (21.1), which differs from the general tendency for a trade-off between refractive index and Abbe number. This work demonstrates the great potential of DESs for the sustainable production of next-generation high-refractive-index polymers and provides new opportunities for their applications in related fields.

Received 1st November 2025,
Accepted 2nd January 2026

DOI: 10.1039/d5lp00343a

rsc.li/rscapplpolym

Introduction

High-refractive-index polymers are indispensable for a prosperous society with a wide range of applications, such as modern lenses, image sensors, antireflective coatings, microlens arrays, and optical guides.[1–8] The structural design and practical synthesis of polymers with high refractive indices, particularly those higher than 1.7, have attracted significant interest, and generally rely on building blocks with high molar refraction and small molar volume, based on the Lorentz–Lorenz equation.[1–3,7,9] For instance, sulfur atoms have been incorporated in polymeric materials using various modern methods, such as thiol–ene[10–16] and thiol–yne[17,18] reactions, ring-opening polymerization,[19] and inverse-vulcanization.[7,20] Other intriguing examples involve the incorporation of high molar refraction units (*e.g.*, phosphorus units[21]), highly polarizable atoms (*e.g.*, Ge and Sn),[22] metal (*e.g.*, Zn[23] and Zr[24]), and semimetal (*e.g.*, Se[11,25–27]). The utilization of charge-transfer complexation[28] and hydrogen bonds[29] has recently emerged as an efficient tool for enhancing the refractive index.

Despite continuous progress in synthetic methodologies for high-refractive-index polymers, they are generally produced by polymerization in harmful and volatile organic solvents. Owing to the increasing demand for sustainable production with environmentally friendly systems, the development of a greener process is highly desirable to produce high-refractive-index polymers, in which the environmental impact can be reduced by using fewer organic solvents while achieving high polymerization efficacy (high atom economy). Deep eutectic solvents (DESs) have recently emerged as practical green solvents with unique and attractive properties (*e.g.*, low volatility, non-toxicity, cost effectiveness, thermal stability, low flammability, tunable polarity and solubility).[30–33] A variety of DESs,

[a]*Department of Organic Materials Science, Graduate School of Organic Materials Science, Yamagata University, 4-3-16, Jonan, Yonezawa, 992-8510, Japan. E-mail: h.mori@yz.yamagata-u.ac.jp*
[b]*National Institute for Materials Science, 1-2-1, Sengen, Tsukuba, 305-0047, Japan*

usually obtained by mixing two or more solids corresponding to a hydrogen bond acceptor and donor (HBA and HBD), have been employed as green solvents in various polymerization systems.[34–36] The increased viscosity and polarity of DESs has been reported to enhance the polymerization rate, compared to conventional solvents (*e.g.*, aqueous or organic solvents).[37,38] Among DESs with a wide range of HBA/HBD combinations and structural diversity, natural DESs (NADESs) consisting of natural components (*e.g.*, sugars, organic acids, and amino acids)[33,39,40] have emerged as promising green solvents in various fields, including polymer science.[41] A variety of studies have been reported on the effect of DESs on the polymerization of methyl methacrylate (MMA).[42–44] For instance, Serra *et al.* reported homogeneous radical polymerization of MMA and other hydrophobic monomers in DL-menthol/1-tetradecanol NADES,[42] and block copolymer synthesis using MMA in L-menthol/thymol NADES.[43] Yu *et al.* demonstrated photo-induced reversible addition–fragmentation chain transfer (RAFT) polymerization of MMA in tetrabutylammonium chloride/ethylene glycol DES in air,[44] and the potential of DESs for the production of ultrahigh molecular weight PMMA.[45] However, DESs have rarely been used to produce high-refractive-index polymers.

In this study, we investigated the effect and usefulness of DESs for the sustainable production of high-refractive-index polymers *via* the radical copolymerization of the aromatic heterocyclic *S*-vinyl and *N*-vinyl monomers, benzothiazoyl vinyl sulfide (BTVS) and *N*-vinyl carbazole (NVC), which were selected to enhance the refractive index (Fig. 1a). As a comonomer, MMA was also selected, owing to its use as a starting monomer for the production of PMMA thermoplastic known as organic glass or acrylate glass (refractive index = 1.49 and Abbe number = 58).[3,6] Remarkably high molar refraction of the –C═N–C– group (4.10), compared to that of the –C═C–C– group (1.73),[46] enables aromatic heterocycles to act as efficient building blocks to enhance the refractive index of synthetic polymers, *e.g.*, triazines,[47–49] pyridazines,[50] pyrimidines[50–52] and carbazole[16] units in the backbone chains, as well as carbazole,[6,53] thiophene,[54,55] and thiadiazole[1,56] units in the side chains. We previously reported the effectiveness of *S*-vinyl sulfides with aromatic heterocycles (*e.g.*, BTVS) for the production of high-refractive-index polymers,[57,58] owing to their high sulfur content, –C═N– bonds, and aromatic rings in the monomer units. However, synthetic difficulties were occasionally encountered in achieving high molecular weight products, complete monomer conversion (high polymer yield), and a limited range of suitable comonomers because of the relatively low polymerizability of *S*-vinyl monomers. For instance, radical polymerization of BTVS, which has two sulfur atoms, one –C═N–C– group, and one benzene ring, afforded PBTVS with a high refractive index (1.7432, Abbe number = 17.0),[57] whereas the monomer conversion and molecular weights were limited even in bulk polymerization.[59] Block and random copolymers consisting of BTVS with 2-vinylnaphthalene prepared by RAFT polymerization in dimethyl formamide (DMF) allowed for the improvement of transparency while maintaining a high refractive index (1.72–1.66).[57] Nevertheless, a greener and more efficient methodology enabling simul-

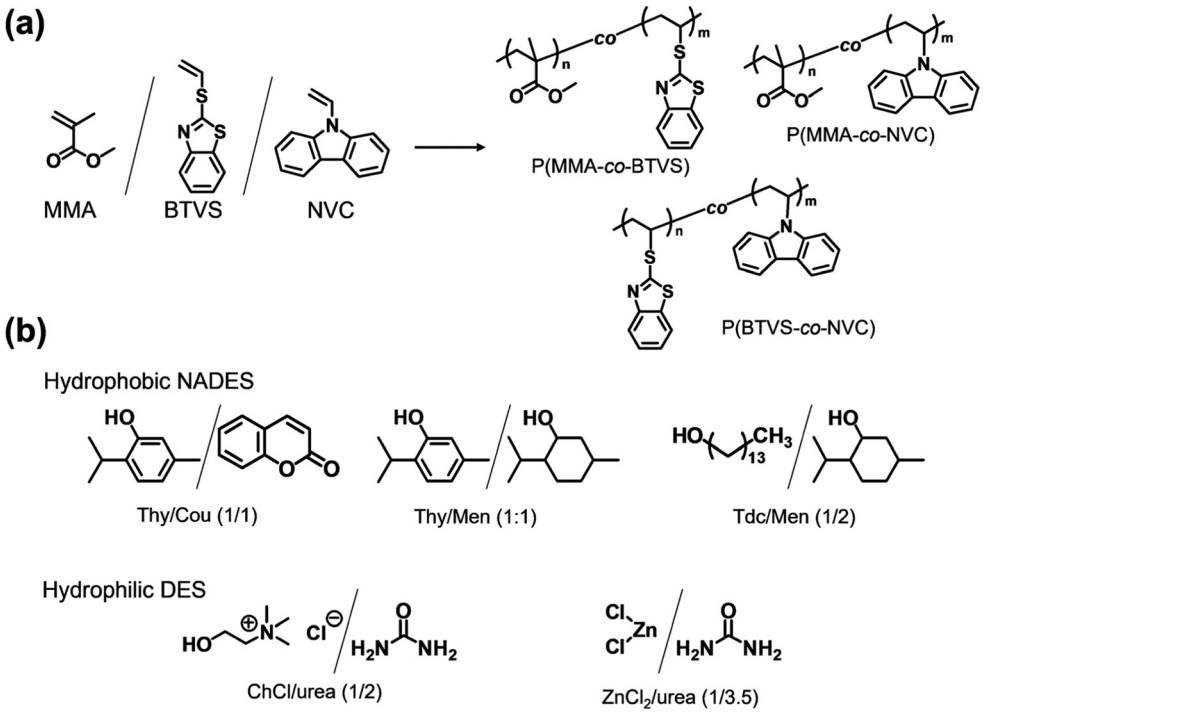

Fig. 1 Synthesis of (a) high-refractive-index copolymers by radical copolymerization of aromatic heterocyclic *S*-vinyl and *N*-vinyl monomers and (b) structures of hydrophobic NADESs and hydrophilic DESs. The number in the parentheses corresponds to the feed ratio.

taneous achievement of high-refractive-index polymers with improved productivity (*e.g.*, higher conversion) and other essential properties (*e.g.*, high Abbe number, high transparency) is still required.

In this study, three hydrophobic NADESs (Thy/Cou (1/1), Thy/Men (1/1), and Tdc/Men (1/2)) prepared from naturally derived compounds (Thy: thymol, Men: (±)-menthol, Cou: coumarin, and Tdc: 1-tetradecanol) were selected to verify the usefulness of radical (co)polymerization of aromatic heterocyclic monomers (Fig. 1). Two hydrophilic DESs prepared from choline chloride (ChCl) and zinc chloride ($ZnCl_2$) (ChCl/urea (1/2) and $ZnCl_2$/urea (1/3.5)) acting as the HBA, combined with urea as the HBD, were also selected. The effects of these hydrophobic NADESs and hydrophilic DESs on the thermal copolymerization of MMA/BTVS, MMA/NVC, and BTVS/NVC were investigated for their polymerization behavior (improved productivity with higher polymer yield and enhanced molecular weights), optical properties (refractive index, Abbe number, and transparency), and other essential properties (thermal stability and film-forming ability) of the resulting copolymers. Photopolymerization was performed to confirm the extensibility of the DES-based green process. The comonomer combinations and their compositions were optimized to afford targeted high-refractive-index copolymers with reasonable Abbe numbers by tuning the contents of three cardinal units (sulfur, –C═N–, and aromatic units) in the copolymers, while higher molecular weight products with high polymer yield (high productivity) were achieved by suitable selection of the nature of DESs (hydrophobic NADESs and hydrophilic DESs) and polymerization systems (thermal- and photo-induced systems). This study is the first example of the productive integration of DESs and radical copolymerization of aromatic heterocyclic *S*-vinyl and *N*-vinyl monomers toward green and efficient production of high-refractive-index copolymers with improved productivity (polymer yield) and high molecular weights, as well as enhanced refractive indices and Abbe numbers.

Results and discussion

Copolymer synthesis in deep eutectic solvents (DESs)

Three hydrophobic NADESs (Thy/Cou (1/1), Thy/Men (1/1), and Tdc/Men (1/2)) with relatively low viscosities (<100 mPa s)[60] were prepared from naturally derived compounds (Thy, Men, Cou, and Tdc) at suitable feed ratios, as reported previously.[60,61] Two hydrophilic DESs (ChCl/urea (1/2)[30] and $ZnCl_2$/urea (1/3.5)[62]) were also prepared from ChCl and $ZnCl_2$, acting as HBA, combined with urea as HBD, which have relatively high viscosities (750 and 11 340 mPa s for ChCl/urea (1/2) and $ZnCl_2$/urea (1/3.5) at 25 °C (ref. 32)). Liquid MMA was miscible with all the DESs, whereas liquid BTVS was miscible only with Thy/Cou and Thy/Men. Solid NVC was dissolved only in Thy/Cou and Thy/Men. All homopolymers (PMMA, PBTVS, and PNVC) were soluble in Thy/Cou and Thy/Men but insoluble in other DESs (Tdc/Men, ChCl/urea, and $ZnCl_2$/urea), as shown in Table S1. These hydrophobic NADESs and hydrophilic DESs were tested for the radical copolymerization of MMA/BTVS, MMA/NVC, and BTVS/NVC, allowing the production of targeted copolymers with predetermined structures and compositions by selecting comonomer combinations and their feed ratios.

Initially, three hydrophobic NADESs were tested for the thermal radical copolymerization of MMA and BTVS (Table 1). When liquid BTVS was mixed with MMA in the presence of 2,2′-azobis(isobutyronitrile) (AIBN) at $[AIBN]_0/[MMA]_0/[BTVS]_0$ = 1/100/100 in hydrophobic NADESs (conc. = 50 wt%), a transparent solution was obtained, and this transparency was maintained during the copolymerization at 60 °C for 24 h (Fig. S4). The resulting mixture was precipitated in hexane, followed by filtration, yielding P(MMA-*co*-BTVS). ^{1}H NMR spectroscopy of the resulting P(MMA-*co*-BTVS) showed no detectable peaks attributable to NADESs or residual monomers (MMA and BTVS), implying efficient purification (Fig. S3). The polymer yields of P(MMA-*co*-BTVS) prepared in the hydrophobic NADESs (32–55%) were comparable to or higher than those prepared in bulk (34%), suggesting the feasibility of improving productivity using the naturally derived green solvents. Size-exclusion chromatography (SEC) measurements of P(MMA-*co*-BTVS)s revealed a broad unimodal peak with a molecular weight range (number average molecular weight (M_n) = 11 000–19 000, M_w/M_n = 1.91–2.94) lower than that prepared in bulk (M_n = 44 000, M_w/M_n = 2.86). The copolymer structures evaluated using ^{1}H NMR spectroscopy displayed broad peaks corresponding to the aromatic rings of BTVS at 6.5–8.0 ppm and the methoxy group of MMA at approximately 3.5 ppm. The BTVS content in P(MMA-*co*-BTVS)s determined by elemental analysis was 32–44%, suggesting the preferred insertion of MMA. This tendency is attributed to the reactivities of MMA (Q = 0.74, e = 0.40 (ref. 63)) and the BTVS derivative (Q = 0.32, e = −1.4 (ref. 64) for phenyl vinyl sulfide). These results are consistent with our preliminary experimental results of thermal homopolymerization in hydrophobic NADESs (Tables S3 and S5, Fig. S1 and S2), showing the formation of high molecular weight PMMA with relatively high conversion (*e.g.*, M_n = 120 000, yield = 64%), whereas in the case of BTVS there was a lower molecular weight and conversion (*e.g.*, M_n = 5400, yield = 20%) in Tdc/Men.

When hydrophilic DESs (ChCl/urea and $ZnCl_2$/urea) were used for the copolymerization of MMA and BTVS under the same conditions ($[AIBN]_0/[MMA]_0/[BTVS]_0$ = 1/100/100, conc. = 50 wt%), it was difficult to achieve a miscible state with BTVS in DES (Table S1), leading to heterogeneous polymerization at 60 °C for 24 h (Fig. S4). Using an efficient purification process by reprecipitation into methanol, the hydrophilic DESs and unreacted monomers (MMA and BTVS) could be removed, as confirmed by ^{1}H NMR spectroscopy (Fig. S3). Under these conditions, copolymerization proceeded efficiently to afford P(MMA-*co*-BTVS)s as white solids with higher yields (59–67%) and molecular weights (M_n = 51 000–85 000, M_w/M_n = 2.75–2.73) than those in bulk. This may be due to the higher viscosity of the hydrophilic DESs, which leads to a relatively

Table 1 Thermal radical copolymerization of aromatic heterocyclic monomers in DESs[a]

Entry	Monomer (M_1/M_2)	$[I]_0/[M_1]_0/[M_2]_0$	DES	Yield[b] (%)	M_n [c] (SEC)	M_w/M_n [c] (SEC)	$n:m$[d]
CP1-1	MMA/BTVS	1/100/100	Bulk	34	44 000	2.86	50 : 50
CP1-2			Thy/Cou	32	11 000	1.91	68 : 32
CP1-3			Thy/Men	38	14 000	2.19	60 : 40
CP1-4			Tdc/Men	55	19 000	2.94	56 : 44
CP1-5			ChCl/urea	67[e]	85 000	2.73	54 : 46
CP1-6			$ZnCl_2$/urea	59[e]	51 000	2.75	44 : 56
CP2-1	MMA/NVC	1/100/100	Bulk	76	60 000	4.39	46 : 54[f]
CP2-2			Thy/Cou	60	56 000	3.07	69 : 31[f]
CP2-3			Thy/Men	<5%	—	—	—
CP2-4			Tdc/Men	82	59 000	2.80	54 : 46[f]
CP2-5			ChCl/urea	85[e]	95 000	2.82	35 : 65[f]
CP2-6			$ZnCl_2$/urea	61[e]	250 000	2.52	58 : 42[f]
CP3-1	BTVS/NVC	1/100/100	Bulk	13	680	1.82	9 : 91
CP3-2			Thy/Cou	21	750	1.61	1 : 99
CP3-3			Tdc/Men	14	3900	1.89	83 : 17
CP3-4			ChCl/urea	50[e]	18 000	2.29	69 : 31
CP3-5			$ZnCl_2$/urea	33[e]	5500	4.33	58 : 42
CP3-6		1/50/150	$ZnCl_2$/urea	34[e]	3300	7.71	34 : 66
CP3-7		1/75/125	$ZnCl_2$/urea	38[e]	4300	6.67	51 : 49
CP3-8		1/150/50	$ZnCl_2$/urea	32[e]	8400	3.57	89 : 11

[a] Copolymerization with AIBN in DES at 60 °C for 24 h. [b] Hexane insoluble part. [c] Measured by SEC using PSt standard in DMF. [d] Evaluated from sulfur content determined by elemental analysis. [e] Methanol insoluble part. [f] Evaluated from nitrogen content determined by elemental analysis.

slow diffusion of radical species, and therefore a decrease in chain transfer and termination reactions, resulting in higher molecular weights and polymer yields. Another hypothesis is the protected radical effect, by which small monomer domains are formed with DES, like the case of ionic liquids, to reduce the termination rate, resulting in increased molecular weights, and increase the concentration of radicals, leading to the increased polymer yields.[44,65] The copolymerization at higher temperature (80 °C) led to a slight decrease in the molecular weights (M_n = 40 000–29 000, Table S7).

Photopolymerization of MMA and BTVS was also attempted using hydrophobic NADESs (Table S8). A homogeneous mixture was obtained from liquid MMA and BTVS in the presence of a photoinitiator (2,2-dimethoxy-2-phenylacetophenone (DMPA)) at $[DMPA]_0/[MMA]_0/[BTVS]_0$ = 1/100/100 in hydrophobic NADESs (50 wt%). The copolymerization was performed using UV light (λ = 365 nm, 330 mW cm^{-2} for LED light) at room temperature in air. Copolymerization proceeded homogeneously in Thy/Cou and Thy/Men, whereas heterogeneous copolymerization occurred for Tdc/Men. P(MMA-*co*-BTVS)s with relatively low yields (30–36%) and molecular weights (M_n = 8200–8400, M_w/M_n = 2.21–4.62) were obtained, regardless of the NADESs, suggesting a limited effect of the nature of the NADESs on the photocopolymerization behavior. A similar tendency was also observed in photohomopolymerization in hydrophobic NADESs (yield = 14–34% for BTVS and 6–16% for MMA, Tables S4 and S6). Photocopolymerization in hydrophilic DESs is impossible because of insufficient solubility of the monomers (MMA and BTVS) in hydrophilic DESs at room temperature (Table S1). Nevertheless, these results imply the feasibility of using nonvolatile DESs for the photopolymerization of aromatic heterocyclic monomers, which can extend the possibility of producing high-refractive-index polymers for a broad range of potential applications such as nanoimprinting and 3D printing under ambient conditions.

Solid *N*-vinyl monomer (NVC) was copolymerized with liquid MMA in DESs (Table 1). Under copolymerization conditions of $[AIBN]_0/[MMA]_0/[NVC]_0$ = 1/100/100, solid NVC was dissolved in liquid MMA at room temperature prior to carrying out bulk copolymerization. The results were compared to copolymerization in DESs (Table 1). When the copolymerization was conducted in the hydrophobic NADESs (Thy/Cou and Tdc/Men) with AIBN at 60 °C for 24 h, P(MMA-*co*-NVC)s with higher yields (60–82%) and molecular weights (M_n = 56 000–59 000, M_w/M_n = 2.80–3.07) were obtained, which were comparable to those in the bulk copolymerization (yield = 76%, M_n = 60 000, M_w/M_n = 4.39). A remarkably high molecular weight P(MMA-*co*-NVC) (M_n = 250 000) was obtained in $ZnCl_2$/urea, and a relatively high molecular weight product with high yield (M_n = 95 000, yield = 85%) was obtained in ChCl/urea, implying that the nature of the hydrophilic DES can contribute to an increase in the molecular weight and polymer yield. The photocopolymerization of MMA and NVC afforded P(MMA-*co*-NVC) with moderate molecular weight and polymer yield (M_n = 11 100, yield = 61%) in Thy/Men (Table S8). This behavior was distinct from that of thermal copolymerization, showing no significant P(MMA-*co*-NVC) was obtained with AIBN at 60 °C (yield < 5%, Table 1). These results imply the feasibility of using both thermo- and photo-induced systems, depending on the nature of the aromatic heterocyclic monomers and constitutional components of the DESs, for the production of targeted high-refractive-index copolymers.

The effects of hydrophobic NADESs and hydrophilic DESs on the copolymerization of BTVS and NVC with AIBN were studied under the same conditions (Table 1). Even when solid NVC was dissolved in liquid BTVS, bulk copolymerization of BTVS and NVC at 60 °C afforded only oligomers (M_n < 1000) with a low yield (13%). A similar low molecular weight P(BTVS-*co*-NVC) was obtained in hydrophobic NADESs. A remarkable increase in the polymer yield and molecular weight of P(BTVS-*co*-NVC) was achieved by copolymerization in hydrophilic DESs; the highest molecular weight P(BTVS-*co*-NVC) (M_n = 18 000, M_w/M_n = 2.29) was obtained with high yield (50%) in ChCl/urea, and a relatively high molecular weight product with broad molecular weight distribution (M_n = 5500, M_w/M_n = 4.33) was obtained in $ZnCl_2$/urea at 60 °C. The resulting BTVS/NVC copolymers were insoluble in the hydrophilic DESs, and therefore liquid BTVS and solid NVC monomers were suspended during polymerization. Similar to emulsion polymerization, the polymerization rate (R_p) is substantially higher in the hydrophilic DESs (heterogeneous system) than in the hydrophobic NADESs (homogeneous system), which is probably attributed to compartmentalization effect. The segregation of the propagating radicals in a compartmentalized system may lead to a reduced termination rate. Such behaviors may affect the improved yields and molecular weights. The copolymerization of BTVS and NVC at higher temperature (80 °C) led to a slight decrease in the molecular weight (M_n < 10 000), regardless of the hydrophobic NADESs and hydrophilic DESs (Table S7).

To find a suitable composition in terms of the polymerization behavior (polymer yield and molecular weights) and optical properties (high refractive index, high Abbe number, film-forming ability, and transparency), copolymerization was conducted at 60 °C in hydrophilic $ZnCl_2$/urea at different feed ratios ($[BTVS]_0/[NVC]_0$ = 50/150, 75/125, and 150/50). The SEC traces of the copolymers showed bimodal peaks or a broad peak with a tailing at lower molecular weight region (Fig. S14a). Nevertheless, P(BTVS-*co*-NVC)s with high weight average molecular weights (M_w > 20 000) and different comonomer compositions were obtained (Table 1) depending on the feed ratio. Hence, the copolymerization strategy in DESs affords a greener and more efficient methodology to overcome the inherent synthetic drawbacks (low productivity and insufficient molecular weights) of copolymers consisting of aromatic heterocyclic *S*-vinyl and *N*-vinyl monomers.

Correlation between refractive indices and Abbe numbers

To evaluate the differences between the three series of MMA/BTVS, MMA/NVC, and BTVS/NVC copolymers, their sulfur and nitrogen contents, refractive indices, and Abbe numbers are summarized in Table 2. All the copolymers, P(MMA-*co*-BTVS), P(MMA-*co*-NVC), and P(BTVS-*co*-NVC), exhibit good solubility in common solvents (*e.g.*, $CHCl_3$ and DMF, Table S10), affording good processability and film-forming ability, such as the formation of smooth thin films *via* a spin-coating process. This good solubility likely originates from the molecular design of the aromatic heterocyclic monomers, which have flexible C–S bonds in BTVS and C–N bonds in NVC, leading to free rotation between the C–C backbone chain and heterocycle-substituted pendant groups in the copolymers. Uniform thin films of P(MMA-*co*-BTVS), P(MMA-*co*-NVC), and P(BTVS-*co*-NVC) were prepared by spin coating $CHCl_3$ solutions (conc. = 1.0 wt%, 1500 rpm, 90 s), which were used for ellipsometry measurements. Fig. 2 compares the wavelength-dependent refractive indices of P(MMA-*co*-BTVS), P(MMA-*co*-NVC), and P(BTVS-*co*-NVC) prepared at a constant feed ratio (100/100) in hydrophobic NADESs, hydrophilic DESs, and bulk. The P(MMA-*co*-BTVS)s with high molecular weights prepared in

Table 2 Characteristics and optical properties of aromatic heterocycle-containing copolymers[a]

Entry[b]	S cont.[c] (%)	N cont.[d] (%)	Film thickness (nm)	n_D (589 nm)	n_F (486 nm)	n_d (587 nm)	n_c (656 nm)	ν_D
CP1-1	21.70	4.76	131.5	1.6488	1.6696	1.6491	1.6423	23.8
CP1-2	15.74	5.17	96.6	1.6076	1.6233	1.6077	1.6039	31.2
CP1-3	18.63	4.04	106.2	1.6159	1.6320	1.6160	1.6118	30.5
CP1-4	19.87	4.30	107.5	1.6253	1.6425	1.6255	1.6210	29.1
CP1-5	20.60	4.68	191.9	1.6794	1.7044	1.6797	1.6690	19.2
CP1-6	23.45	5.07	114.5	1.6443	1.6663	1.6446	1.6376	22.5
CP2-1	—	5.03	178.5	1.6349	1.6679	1.6353	1.6209	13.5
CP2-2	—	3.39	136.2	1.5922	1.6124	1.5924	1.5846	21.3
CP2-6	—	4.22	263.0	1.6065	1.6244	1.6067	1.6021	27.2
CP3-1	3.04	7.20	97.6	1.6822	1.7115	1.6825	1.6752	18.8
CP3-2	0.37	6.72	101.0	1.6738	1.7028	1.6741	1.6668	18.7
CP3-3	27.35	6.87	86.1	1.7141	1.7407	1.7144	1.7063	20.8
CP3-4	22.83	7.51	109.2	1.7359	1.7598	1.7361	1.7301	24.8
CP3-5	19.36	7.20	101.5	1.7204	1.7471	1.7206	1.7141	21.9
CP3-6	11.32	7.97	114.1	1.7193	1.7476	1.7195	1.7134	21.0
CP3-8	29.40	7.29	117.1	1.7528	1.7811	1.7531	1.7454	21.1
CP3-11	23.42	7.19	113.8	1.7172	1.7465	1.7175	1.7081	18.7

[a] Film thickness, refractive indices (n_D, n_F, n_d, and n_c) and Abbe number (ν_D) were determined by ellipsometry. [b] See Table 1 and Table S7 for detailed copolymer samples. CP1, CP2, and CP3 correspond to P(MMA-*co*-BTVS), P(MMA-*co*-NVC), and P(BTVS-*co*-NVC), respectively. [c] Sulfur content. [d] Nitrogen content.

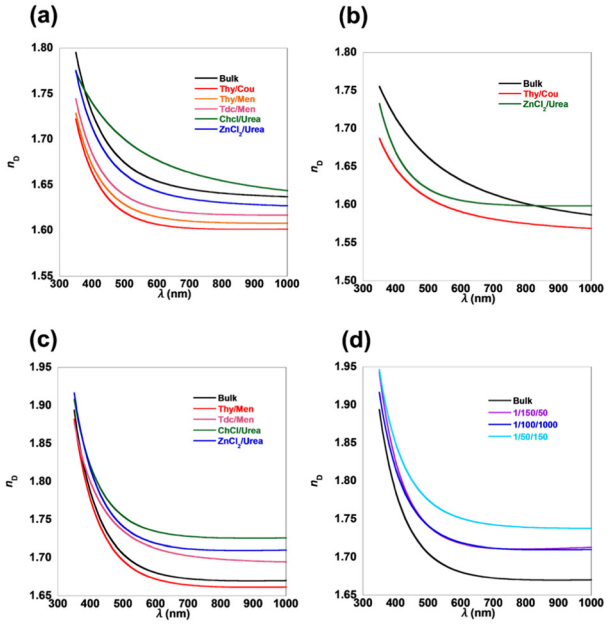

Fig. 2 Wavelength-dependent refractive indices of the copolymer films, (a) P(MMA-*co*-BTVS)s, (b) P(MMA-*co*-NVC)s, and (c) P(BTVS-*co*-NVC)s prepared at a constant feed ratio (100/100) in different DESs, and (d) P(BTVS-*co*-NVC)s prepared at different feed ratios in $ZnCl_2$/urea.

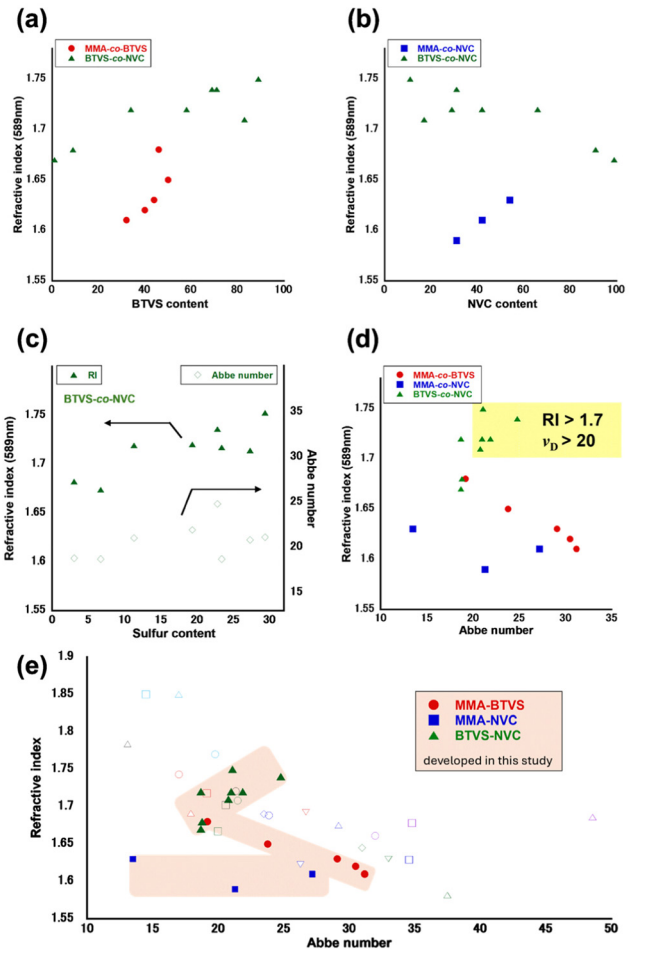

Fig. 3 Correlations between (a) refractive index and BTVS content for BTVS-containing copolymers, (b) refractive index and NVC content for NVC-containing copolymers, (c) refractive index, Abbe number, and sulfur content for P(BTVS-*co*-NVC)s, and (d) refractive index and Abbe number for all copolymers. (e) Comparison between aromatic heterocycle-containing copolymers developed in this work and previously reported polymers (see Table S11 for detailed sample information).

hydrophilic DESs show high refractive indices (1.6794 for ChCl/urea and 1.6443 for $ZnCl_2$/urea), which are comparable to those prepared in bulk (1.6488) and higher than those prepared in hydrophobic NADESs (<1.63). Similarly, P(MMA-*co*-NVC) prepared in $ZnCl_2$/urea shows a higher refractive index (1.6065) than that prepared in Thy/Cou, while the copolymer prepared by bulk polymerization has a higher NVC content and therefore a higher refractive index (1.6349). P(MMA-*co*-BTVS)s show slightly higher refractive indices in the 1.6076–1.6794 range than P(MMA-*co*-NVC)s (1.5922–1.6349), which is likely because of the higher refractive index of BTVS over that of NVC (1.74 for PBTVS,[57] 1.69 for PNVC,[66] and 1.49 for PMMA[3]). Among the three series of copolymers MMA/BTVS, MMA/NVC, and BTVS/NVC, P(BTVS-*co*-NVC)s prepared in hydrophilic DESs show higher refractive indexes (1.7359–1.7204). Both BTVS and NVC contain aromatic heterocycles; consequently, these copolymers exhibit excellent refractive indices.

As shown in Fig. 3a and b, the refractive index tends to increase with increasing BTVS and NVC content in P(MMA-*co*-BTVS)s and P(MMA-*co*-NVC)s, respectively. The Abbe numbers of MMA-containing copolymers vary substantially in the 19–32 range for P(MMA-*co*-BTVS)s and 13–28 for P(MMA-*co*-NVC)s, depending on the MMA content. These results are consistent with the general tendency that an increase in the refractive index leads to a decrease in the Abbe number. However, achieving high refractive indices while maintaining a high Abbe number is challenging; a lower Abbe number corresponds to higher dispersion.[1,2] The refractive indices of the P(BTVS-*co*-NVC)s with different comonomer compositions increase substantially with increasing BTVS content (Fig. 3a). The contents of three cardinal units (sulfur, –C═N–, and aromatic rings) in the P(BTVS-*co*-NVC)s were determined by tuning the BTVS feed ratio, and refractive indices of P(BTVS-*co*-NVC)s increased from 1.6738 to 1.7528, while maintaining Abbe numbers greater than 18. As shown in Fig. 3c, the Abbe numbers of P(BTVS-*co*-NVC)s (18–25) are less sensitive to the sulfur content. This is attributed to the similar characteristics of BTVS and NVC, which are aromatic heterocyclic vinyl monomers with S and N atoms that are inherently distinct from conventional monomers containing only carbon and oxygen atoms (*e.g.*, MMA). Notably, P(BTVS-*co*-NVC)s having suitable comonomer compositions (BTVS/NVC = 89/11–34/66) exhibit refractive indices of higher than 1.7 and Abbe numbers greater than 20, which differs from the general tendency for a trade-off between the refractive index and Abbe number (Fig. 3d). Comparison between aromatic heterocycle-containing copolymers developed in this work and previously reported polymers

also indicates unique tendency of P(BTVS-*co*-NVC)s (Fig. 3e and Table S11), suggesting the possibility to go beyond a limitation line for the trade-off between the refractive index and Abbe number. Particularly, P(BTVS-*co*-NVC) prepared with $[BTVS]_0/[NVC]_0$ = 150/50 in $ZnCl_2$/urea shows the highest refractive index (1.7528) with a relatively high Abbe number (21.1). In contrast, a typical trade-off between the refractive index and Abbe number is observed for P(MMA-*co*-BTVS)s and the refractive indexes of P(MMA-*co*-NVC)s are less sensitive to the Abbe numbers (Fig. 3e). In addition to the high molar fractions of both BTVS and NVC, which have aromatic heterocycles, the high refractive indices of the P(BTVS-*co*-NVC)s can be attributed to low molar volumes governed by polymerization shrinkage. Generally, a polymer exhibits a higher refractive index than that of the corresponding monomer because of denser packing.[6] In our system, two vinyl monomers were copolymerized radically, which led to the loss of a double bond for each monomer, resulting in shrinkage. The decrease in the molar volume *via* shrinkage during copolymerization may contribute to the high refractive indices of P(BTVS-*co*-NVC)s, and the degree of the shrinkage is probably affected by the comonomer feed ratio and polymerization conditions (*e.g.*, employment of DESs). Because the Abbe number is determined by the refractive index in addition to the molar refraction and molar dispersion,[1,2] shrinkage during copolymerization may affect the Abbe number. The unique characteristics of DESs, their ability to form hydrogen bonds, and other specific interactions with monomers (*e.g.*, thiazoyl group in BTVS, carbazole unit in NVC, and ester group in MMA), may contribute to improving the polymer yield and molecular weights, and to solving the tendency for a trade-off between refractive index and Abbe number.

Optical and thermal properties

The simultaneous achievement of high refractive index, high Abbe number, good transparency, and high thermal stability is still a target of interest in the field of high-refractive-index polymers. The transparency of the representative copolymers, P(MMA-*co*-BTVS), P(MMA-*co*-NVC), and P(BTVS-*co*-NVC), with similar comonomer compositions, was evaluated using UV-vis spectrophotometry. The combination-dependent transparency and thermal stability of the comonomers are compared in Table 3. Copolymer films produced by drop-casting from a $CHCl_3$ solution (1.0 wt%) were used for evaluation, and the results are shown in Fig. 4a. Three copolymers show good transparency in the visible region (>96% at 400 nm), regardless of the comonomer combination (MMA/BTVS, MMA/NVC, or BTVS/NVC). As expected, radical copolymerization of MMA with the aromatic heterocyclic monomers afforded copolymers with good transparency, film-forming ability, and high thermal stability originating from MMA incorporation while maintaining a relatively high refractive index. Furthermore, structural design of pendant type copolymers with free rotation between the C–C backbone chain and aromatic heterocycle-substituted pendant groups can efficiently reduce interactions between the aromatic heterocycles and delocalized π-electrons. The incorporation of suitable aromatic heterocycles into the side chain through flexible C–S and C–N bonds impart good solubility and film-forming ability under mild conditions, in addition to an enhanced refractive index and Abbe number. No significant effect of the yellow color on the interpretation of optical measurements was detected for P(BTVS-*co*-NVC)s, while the cause of the yellow coloration is unknown. Further studies to clarify the cause of the coloring and to provide a suitable method for preventing yellow coloration are now in progress and will be communicated separately.

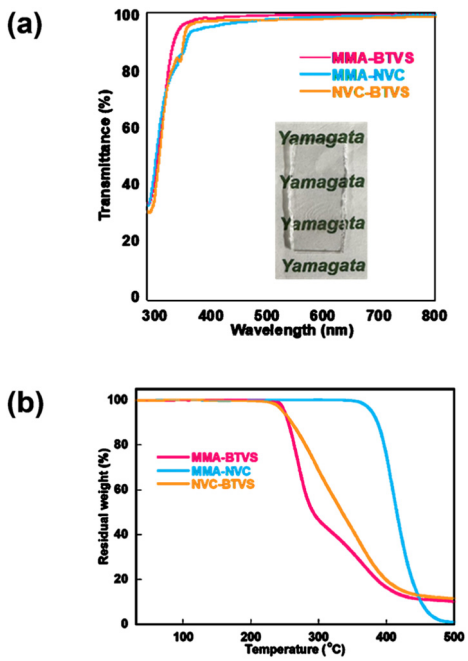

Fig. 4 (a) UV-vis transmittance spectra and photographs of representative copolymer films and (b) TGA curves of the representative copolymers, P(MMA-*co*-BTVS), P(MMA-*co*-NVC), and P(BTVS-*co*-NVC).

Table 3 Characteristics of aromatic heterocycle-containing copolymers[a]

Entry	Sample	M_n [b] (M_w/M_n)	n/m[c]	Sulfur cont.[c]	Film thickness[d] (nm)	RI[d]	Abbe number[d]	T_{d5} [e] (°C)
CP1-5	P(MMA-*co*-BTVS)	85 000 (2.73)	54 : 46	20.60	191.9	1.6794	19.2	249
CP2-6	P(MMA-*co*-NVC)	250 000 (2.52)	58 : 42	—	263.0	1.6065	27.2	378
CP3-5	P(BTVS-*co*-NVC)	5500 (4.33)	58 : 42	19.36	101.5	1.7204	21.9	246

[a] See Table 1 for detailed copolymer samples. [b] Measured by SEC. [c] Determined by elemental analysis. [d] Determined by ellipsometry. [e] The temperature at 5% weight loss (T_{d5}).

Thermogravimetric analysis (TGA) of P(MMA-*co*-BTVS) and P(BTVS-*co*-NVC) reveals a gradual and/or stepwise thermolysis process in the range of 240–400 °C, whereas P(MMA-*co*-NVC) shows single-step decomposition in the range of 370–460 °C, as shown in Fig. 4b. The T_{d5} of P(MMA-*co*-NVC) is 378 °C, which is significantly higher than those of P(MMA-*co*-BTVS) and P(BTVS-*co*-NVC) (T_{d5} = 249 °C and 246 °C, respectively). Glass transition temperature (T_g) values of representative P(MMA-*co*-NVC)s were 153–158 °C, which were determined by differential scanning calorimetry (DSC). The values were apparently higher than those of BTVS-containing copolymers (T_g = 87–103 °C for P(MMA-*co*-BTVS)s and 88–90 °C for P(BTVS-*co*-NVC)s, Fig. S15). The thermal properties (T_{d5} and T_g values) could be manipulated by the chemical structure of the monomers, their composition, and molecular weights, which are crucial for further investigations (*e.g.*, mechanical properties measurement). High thermal stability and practical optical transparency of P(MMA-*co*-NVC), while maintaining relatively high refractive indices (1.59–1.64), are attributed to suitable incorporation of MMA in the copolymers. P(BTVS-*co*-NVC)s synthesized from two aromatic heterocyclic monomers in DESs exhibit sufficient thermal stability (T_{d5} > 240 °C), highest refractive index (>1.7), relatively high Abbe number (>20), and high transparency (>96% at 400 nm), which make them promising candidates for future green production of high-refractive-index copolymers.

Conclusion

Three series of copolymers were synthesized by radical copolymerization of aromatic heterocyclic monomers (BTVS and NVC), combined with MMA, in hydrophobic NADESs and hydrophilic DESs. Compared with a conventional strategy using organic solvents or in bulk, radical copolymerization in DES has the following advantages: (i) increase in productivity (*e.g.*, higher polymer yields of P(MMA-*co*-BTVS) prepared in ChCl/urea and Tdc/Men, and P(BTVS-*co*-NVC) prepared in ChCl/urea, compared to those in bulk), (ii) increase in molecular weight (*e.g.*, highest molecular weights of P(MMA-*co*-NVC) prepared in $ZnCl_2$/urea, and P(MMA-*co*-BTVS) and P(BTVS-*co*-NVC) prepared in ChCl/urea), and (iii) increased refractive index (*e.g.*, higher refractive index of P(BTVS-*co*-NVC) prepared in ChCl/urea and $ZnCl_2$/urea). Advantages (i) and (ii) are related to the increased viscosity and polarity of the DESs, depending on their nature. Advantage (iii) is related to the comonomer composition (*e.g.*, BTVS/NVC) and the degree of shrinkage during copolymerization, which are likely affected by the nature of the DESs used as green polymerization solvents. P(BTVS-*co*-NVC) prepared in $ZnCl_2$/urea showed the highest refractive index (>1.75) and a relatively high Abbe number (>21). The green synthetic approach using DESs involves the integration of aromatic heterocyclic *S*-vinyl and *N*-vinyl monomers to increase the refractive index and MMA to achieve good transparency and polymerizability. Suitable combinations of building blocks with aromatic heterocycles and DESs endow high-refractive-index copolymers with high Abbe numbers, high transparency, and increased productivity.

Author contributions

Yuji Tsuhara: investigation, methodology, writing – original draft; Kento Sato: investigation; Sadaki Samitsu: investigation, validation, writing – review & editing; Hideharu Mori: conceptualization, supervision, validation, writing – review & editing.

Conflicts of interest

There are no conflicts of interest to declare.

Data availability

The data supporting this article have been included as part of the supplementary information (SI). Supplementary information: experimental details, preliminary polymerization results in DESs (homopolymerization, copolymerization at higher temperature, and photocopolymerization), photographs of representative samples, and material characterization data (^{1}H NMR spectra, SEC traces, solubility/miscibility, elemental analysis, and DSC results), and comparison data. See DOI: https://doi.org/10.1039/d5lp00343a.

Acknowledgements

This work was financially supported by a JSPS KAKENHI Grant-in-Aids for Scientific Research (B) (23H02007). This work was supported by "Advanced Research Infrastructure for Materials and Nanotechnology in Japan (ARIM)" of the Ministry of Education, Culture, Sports, Science and Technology (MEXT), Proposal Number JPMXP1224NM5511.

References

1 J.-g. Liu and M. Ueda, *J. Mater. Chem.*, 2009, **19**, 8907–8919.
2 T. Higashihara and M. Ueda, *Macromolecules*, 2015, **48**, 1915–1929.
3 G. S. Jha, G. Seshadri, A. Mohan and R. K. Khandal, *e-Polym.*, 2007, 120.
4 H. Ma, A. K. Y. Jen and L. R. Dalton, *Adv. Mater.*, 2002, **14**, 1339–1365.
5 D. Helmut, *Angew. Chem., Int. Ed. Engl.*, 1979, **18**, 49–59.
6 T. Badur, C. Dams and N. Hampp, *Macromolecules*, 2018, **51**, 4220–4228.
7 T. S. Kleine, R. S. Glass, D. L. Lichtenberger, M. E. Mackay, K. Char, R. A. Norwood and J. Pyun, *ACS Macro Lett.*, 2020, **9**, 245–259.
8 K. Mazumder, B. Voit and S. Banerjee, *ACS Omega*, 2024, **9**, 6253–6279.

9 E. K. Macdonald and A. P. Shaver, *Polym. Int.*, 2015, **64**, 6–14.
10 X. Chen, L. Fang, J. Wang, F. He, X. Chen, Y. Wang, J. Zhou, Y. Tao, J. Sun and Q. Fang, *Macromolecules*, 2018, **51**, 7567–7573.
11 Y. Su, E. B. D. S. Filho, N. Peek, B. Chen and A. E. Stiegman, *Macromolecules*, 2019, **52**, 9012–9022.
12 M. D. Alim, S. Mavila, D. B. Miller, S. Huang, M. Podgorski, L. M. Cox, A. C. Sullivan, R. R. McLeod and C. N. Bowman, *ACS Mater. Lett.*, 2019, **1**, 582–588.
13 K. Nakabayashi, S. Sobu, Y. Kosuge and H. Mori, *J. Polym. Sci., Part A: Polym. Chem.*, 2018, **56**, 2175–2182.
14 S. Iino, S. Sobu, K. Nakabayashi, S. Samitsu and H. Mori, *Polymer*, 2021, **224**, 123725.
15 K. Nakabayashi, T. Imai, M.-C. Fu, S. Ando, T. Higashihara and M. Ueda, *Macromolecules*, 2016, **49**, 5849–5856.
16 Z. Dou, J. Li, Z. Shi, J. Sun and Q. Fang, *ACS Appl. Polym. Mater.*, 2025, **7**, 5302–5311.
17 Q. Wei, R. Poetzsch, X. Liu, H. Komber, A. Kiriy, B. Voit, P.-A. Will, S. Lenk and S. Reineke, *Adv. Funct. Mater.*, 2016, **26**, 2545–2553.
18 S. Gazzo, G. Manfredi, R. Poetzsch, Q. Wei, M. Alloisio, B. Voit and D. Comoretto, *J. Polym. Sci., Part B:Polym. Phys.*, 2016, **54**, 73–80.
19 M. Luo, X.-H. Zhang and D. J. Darensbourg, *Acc. Chem. Res.*, 2016, **49**, 2209–2219.
20 J. J. Griebel, R. S. Glass, K. Char and J. Pyun, *Prog. Polym. Sci.*, 2016, **58**, 90–125.
21 Z. Tan, C. Wu, M. Zhang, W. Lv, J. Qiu and C. Liu, *RSC Adv.*, 2014, **4**, 41705–41713.
22 S. D. Bhagat, J. Chatterjee, B. Chen and A. E. Stiegman, *Macromolecules*, 2012, **45**, 1174–1181.
23 S. Nagayama and B. Ochiai, *Polym. J.*, 2016, **48**, 1059–1064.
24 S. D. Bhagat, E. B. D. S. Filho and A. E. Stiegman, *Macromol. Mater. Eng.*, 2015, **300**, 580–585.
25 Q. Li, Y. Zhang, Z. Chen, X. Pan, Z. Zhang, J. Zhu and X. Zhu, *Org. Chem. Front.*, 2020, **7**, 2815–2841.
26 Y. Tokushita, A. Watanabe, A. Torii, K. Nakabayashi, S. Samitsu and H. Mori, *React. Funct. Polym.*, 2021, **165**, 104960.
27 Y. Tokushita, S. Furuya, S. Nobe, K. Nakabayashi, S. Samitsu and H. Mori, *Polymer*, 2021, **237**, 124346.
28 N. Huo and W. E. Tenhaeff, *Macromolecules*, 2023, **56**, 2113–2122.
29 S. Watanabe, H. Nishio, T. Takayama and K. Oyaizu, *ACS Appl. Polym. Mater.*, 2023, **5**, 2307–2311.
30 A. P. Abbott, G. Capper, D. L. Davies, R. K. Rasheed and V. Tambyrajah, *Chem. Commun.*, 2003, **1**, 70–71.
31 Q. Zhang, K. D. O. Vigier, S. Royer and F. Jerome, *Chem. Soc. Rev.*, 2012, **41**, 7108–7146.
32 E. L. Smith, A. P. Abbott and K. S. Ryder, *Chem. Rev.*, 2014, **114**, 11060–11082.
33 A. Paiva, R. Craveiro, I. Aroso, M. Martins, R. L. Reis and A. R. C. Duarte, *ACS Sustainable Chem. Eng.*, 2014, **2**, 1063–1071.
34 D. Carriazo, M. C. Serrano, M. C. Gutierrez, M. L. Ferrer and F. del Monte, *Chem. Soc. Rev.*, 2012, **41**, 4996–5014.
35 L. I. N. Tome, V. Baiao, W. da Silva and C. M. A. Brett, *Appl. Mater. Today*, 2018, **10**, 30–50.
36 J. D. Mota-Morales, R. J. Sanchez-Leija, A. Carranza, J. A. Pojman, F. del Monte and G. Luna-Barcenas, *Prog. Polym. Sci.*, 2018, **78**, 139–153.
37 K. F. Fazende, D. P. Gary, J. D. Mota-Morales and J. A. Pojman, *Macromol. Chem. Phys.*, 2020, **221**, 1900511.
38 M. Isik, F. Ruiperez, H. Sardon, A. Gonzalez, S. Zulfiqar and D. Mecerreyes, *Macromol. Rapid Commun.*, 2016, **37**, 1135–1142.
39 Y. H. Choi, J. van Spronsen, Y. Dai, M. Verberne, F. Hollmann, I. W. C. E. Arends, G.-J. Witkamp and R. Verpoorte, *Plant Physiol.*, 2011, **156**, 1701–1705.
40 Y. Dai, J. van Spronsen, G.-J. Witkamp, R. Verpoorte and Y. H. Choi, *Anal. Chim. Acta*, 2013, **766**, 61–68.
41 A. V. Gomez, A. Biswas, C. C. Tadini, R. F. Furtado, C. R. Alves and H. N. Cheng, *J. Braz. Chem. Soc.*, 2019, **30**, 717–726.
42 V. A. Pereira, T. C. Rezende, P. V. Mendonca, J. F. J. Coelho and A. C. Serra, *Green Chem.*, 2020, **22**, 6827–6835.
43 V. A. Pereira, P. V. Mendonca, J. F. J. Coelho and A. C. Serra, *Polymer*, 2022, **242**, 124586.
44 C.-Y. Li and S.-S. Yu, *Macromolecules*, 2021, **54**, 9825–9836.
45 Y.-T. Chou, W.-R. Lee and S.-S. Yu, *Macromolecules*, 2024, **57**, 9241–9249.
46 *Chemical Handbook Basic II*, Maruzen, 1979.
47 Y. Nakagawa, Y. Suzuki, T. Higashihara, S. Ando and M. Ueda, *Macromolecules*, 2011, **44**, 9180–9186.
48 M.-C. Fu, Y. Murakami, M. Ueda, S. Ando and T. Higashihara, *J. Polym. Sci., Part A: Polym. Chem.*, 2018, **56**, 724–731.
49 N.-H. You, T. Higashihara, Y. Oishi, S. Ando and M. Ueda, *Macromolecules*, 2010, **43**, 4613–4615.
50 N.-H. You, Y. Nakamura, Y. Suzuki, T. Higashihara, S. Ando and M. Ueda, *J. Polym. Sci., Part A: Polym. Chem.*, 2009, **47**, 4886–4984.
51 K. Nakabayashi, T. Imai, M.-C. Fu, S. Ando, T. Higashihara and M. Ueda, *J. Mater. Chem. C*, 2015, **3**, 7081–7087.
52 N. Oh, K.-H. Nam, M. Goh, B.-C. Ku, J. G. Kim and N.-H. You, *Polymer*, 2019, **165**, 191–197.
53 R. A. Minns and R. A. Gaudiana, *J. Macromol. Sci., Pure Appl. Chem.*, 1992, **29**, 19–30.
54 Y. C. An and G.-i. Konishi, *J. Appl. Polym. Sci.*, 2012, **124**, 789–795.
55 T. Matsuda, Y. Funae, M. Yoshida and T. Takaya, *J. Macromol. Sci., Pure Appl. Chem.*, 1999, **36**, 1271–1288.
56 Y. Tang, S. Cabrini, J. Nie and C. Pina-Hernandez, *Chin. Chem. Lett.*, 2020, **31**, 256–260.
57 Y. Sato, S. Sobu, K. Nakabayashi, S. Samitsu and H. Mori, *ACS Appl. Polym. Mater.*, 2020, **2**, 3205–3214.
58 I. Watanabe, K. Morikawa, S. Samitsu and H. Mori, *Macromol. Chem. Phys.*, 2023, **224**, 2300289.
59 K. Nakabayashi, A. Matsumura, Y. Abiko and H. Mori, *Macromolecules*, 2016, **49**, 1616–1629.
60 D. J. G. P. van Osch, C. H. J. T. Dietz, J. van Spronsen, M. C. Kroon, F. Gallucci, M. v. S. Annaland and R. Tuinier, *ACS Sustainable Chem. Eng.*, 2019, **7**, 2933–2942.
61 S. Yuki, R. Shinohe, Y. Tanaka and H. Mori, *Polym. Chem.*, 2024, **15**, 3629–3640.

62 A. P. Abbott, J. C. Barron, K. S. Ryder and D. Wilson, *Chem. – Eur. J.*, 2007, **13**, 6495–6501.
63 J. Brandrup and E. H. Immergut, *Polymer Handbook*, Wiley Publisher, New York, 1991.
64 C. C. Price and H. Morita, *J. Am. Chem. Soc.*, 1953, **75**, 4747–4750.
65 K. J. Thurecht, P. N. Gooden, S. Goel, C. Tuck, P. Licence and D. J. Irvine, *Macromolecules*, 2008, **41**, 2814–2820.
66 J. E. McGrath, L. Rasmussen, A. R. Shultz, H. K. Shobha, M. Sankarapandian, T. Glass, T. E. Long and A. J. Pasquale, *Polymer*, 2006, **47**, 4042–4057.